

Short Communication

## Electrochemical Biosensors Based on Carbon Nanocages for the Detection of NADH and Ethanol

Xuyan Mao<sup>1,\*</sup>, Yue wen<sup>2</sup>, Mengling Xiong<sup>2</sup>, Zheng Niu<sup>1</sup>, Liang Jiang<sup>2</sup>,  
Huali Zhang<sup>1</sup>, Lijie Yang<sup>2</sup>, Ruijiao Chen<sup>1,\*</sup>

<sup>1</sup>Collaborat Innovat Ctr Birth Defect Res & Transfo, Jining Medical University, Jining, 272067, Shandong, China.

<sup>2</sup> College of Basic Medicine, Jining Medical University, Jining, 272067, Shandong, China.

\*E-mail: [xuyanm\\_06@163.com](mailto:xuyanm_06@163.com) (Xuyan Mao), [chenrj@mail.jnmc.edu.cn](mailto:chenrj@mail.jnmc.edu.cn) (Ruijiao Chen).

Received: 22 December 2020 / Accepted: 2 February 2021 / Published: 28 February 2021

---

Carbon nanocages (CNCs) were used to prepare modified electrodes and showed excellent electrocatalytic activities in electrochemical catalysis for reduced nicotinamide adenine dinucleotide (NADH). The CNCs-modified glassy carbon electrode (CNCs/GCE) has a high sensitivity to the measurement of NADH ( $15.78 \mu\text{A}\cdot\mu\text{M}^{-1}\cdot\text{cm}^{-2}$ ) and gave a low detection limit of  $0.34 \mu\text{M}$ . An amperometric ethanol biosensor was prepared by combining alcohol dehydrogenase (ADH) with CNCs/GCE. The ethanol biosensor exhibited a wide linear range up to  $5 \text{ mM}$  with a relatively low detection limit of  $0.30 \text{ mM}$  as well as a high sensitivity of  $10.85 \text{ nA/mM}$  without suffering any interference from some common electroactive compounds.

---

**Keywords:** Alcohol dehydrogenase, Biosensors, Ethanol, Carbon Nanocages

### 1. INTRODUCTION

Excessive drinking is a global health problem. Alcohol can spread to various organs of the body, leading to a series of important organ diseases. The liver is the main organ of alcohol metabolism, and excessive drinking can lead to various liver lesions that can eventually develop into primary liver cancer [1]. Studies have shown that the products of ethanol metabolism can directly cause cell damage, and the cytotoxicity increases with increasing ethanol concentration and action time. Therefore, it is necessary to establish a simple, fast and reliable analytical method for the sensitive and selective determination of alcohol. The most important pathway of alcohol metabolism is through two enzymes in the liver, namely, alcohol dehydrogenase (ADH) in the cytoplasm and acetaldehyde dehydrogenase2 [2] (ALDH2) in mitochondria. Nicotinamide adenine dinucleotide ( $\text{NAD}^+$ ) is a coenzyme that receives hydrides, and its reduced state is reduced nicotinamide adenine dinucleotide (NADH), which plays an important role in cell metabolism and energy production, participates in mitochondrial energy

metabolism, and maintains calcium homeostasis, gene expression, oxidative stress, aging and apoptosis [3]. ADH can metabolize ethanol to acetaldehyde. In this process,  $\text{NAD}^+$  is reduced to NADH. The  $\text{NAD}^+/\text{NADH}$  ratio is changed, thus increasing the permeability of the mitochondrial membrane and causing excessive flow of electrons in the respiratory chain, which results in electron accumulation and leakage in mitochondrial respiratory chain complexes I and III, thus producing reactive oxygen species (ROS). Excessive ROS can induce oxidative stress, leading to hepatocyte injury and apoptosis [4]. Therefore, excessive drinking causes great harm to the body. To prevent this injury, we need a fast and simple method to detect the alcohol concentration in the body.

In recent years, carbon nanocages have become one of the most popular carbon nanomaterials. As a novel three-dimensional carbon nanomaterial, CNCs have unique properties and structures, such as low density, high specific surface area, unique porous structure, strong corrosion resistance, good conductivity, and good biocompatibility. Therefore, CNCs are potentially widely used in many aspects, such as hydrogen storage materials, environmental purification, lithium batteries, capacitor materials, drug carriers, protective proteins and catalytic enzymes [5-11]. In recent years, carbon nanocages have been widely used in electrochemical analysis due to their high specific surface area and excellent conductivity. In this paper, cubic carbon nanocages were prepared by the template method and applied to the electrochemical detection of NADH and ethanol, and good results were obtained.

## 2. EXPERIMENTAL SECTION

### 2.1. Reagents

Graphene oxide (GO) dispersion in water was obtained from Jining Leadernano, and sodium borohydride ( $\text{NaBH}_4$ ) was obtained from Alfa Aesar (China).  $\beta$ -Nicotinamide adenine dinucleotide, reduced disodium salt hydrate (NADH), nicotinamide adenine dinucleotide ( $\text{NAD}^+$ ), alcohol dehydrogenase (ADH), Nafion (5% in alcohol), ascorbic acid (AA), dopamine (DA) and uric acid (UA) were obtained from Sigma-Aldrich. All other chemicals were analytical grade and used as received. The aqueous solutions were made with ultrapure water.

### 2.2. Instrumentation

Electrochemical measurements were carried out on a CHI 660E electrochemical workstation (Shanghai Chenhua Instrument Co., Ltd., China). The electrochemical cell was assembled as a traditional three-electrode system. A modified glassy carbon (GC) electrode was used as the working electrode. A coiled platinum wire was used as the counter electrode. All potentials refer to the sodium saturated calomel electrode (SSCE). All electrochemical tests were performed at room temperature (approximately 25 °C).

### 2.3. Procedures

#### 2.3.1. Preparation of CNC and rGO nanomaterials

##### *Preparation of carbon nanocages:*

The preparation method of carbon nanocages is based on that from previously published papers from our laboratory [12]. In the experiment, dry ice was placed in deionized water, and carbon dioxide gas appeared above the beaker. The magnesium strip was ignited in a carbon dioxide atmosphere, and then the sample was leached in hydrochloric acid solution to remove magnesium oxide and unreacted metal magnesium and thoroughly cleaned with deionized water. After that, the sample was dried in an oven at 60 °C to obtain material 1. Material 1 was heated in concentrated nitric acid at 60 °C for 3 hours and then thoroughly cleaned with deionized water to obtain the desired cage-like carbon nanomaterials (CNCs).

##### *Preparation of reduced graphene oxide:*

Seventy-seven milliliters of graphene oxide solution with a concentration of 1.3 mg/ml was used to obtain a uniform GO dispersion by ultrasound for 10 minutes. Sodium borohydride (72.44 mg) was dissolved in 2 ml of deionized water, added to the frozen GO dispersion in an ice bath for 5 minutes, and then stirred at room temperature for 4 hours. The rGO solid powder was obtained by centrifuging at 10000 rpm for 20 minutes, washing three times with deionized water and drying in a vacuum drying oven at 50 °C for 12 hours.

#### 2.3.2. Preparation of CNCs/GC and rGO/GC electrodes

The glassy carbon (GC, 3 mm diameter, CHI 104) electrode was successively polished with alumina slurries of 1.0  $\mu\text{m}$ , 0.3  $\mu\text{m}$  and 0.05  $\mu\text{m}$ , thoroughly cleaned with ultrapure water between the polishing steps, cleaned by ultrasonication in ethanol and deionized water and finally dried in air. Then, 5  $\mu\text{l}$  of the CNC or rGO suspension (1.0 mg  $\text{ml}^{-1}$  in water) was cast onto the surface of the pretreated GC electrode (denoted as CNCs/GC or rGO/GC) with a microsyringe, and the solvent was dried at ambient temperature before use.

#### 2.3.2. Preparation of ADH/CNCs/GC electrodes

The 5% Nafion solution was diluted to 0.5% with PBS (pH 7.0), and 100  $\mu\text{l}$  of the 0.5% Nafion solution was mixed with 1 mg of ADH to obtain the mixture. Five microliters of the mixture was coated on the CNCs/GC electrode with a microinjector and then dried at room temperature.

### 3. RESULTS AND DISCUSSION

#### 3.1. Characterization of CNCs nanomaterials

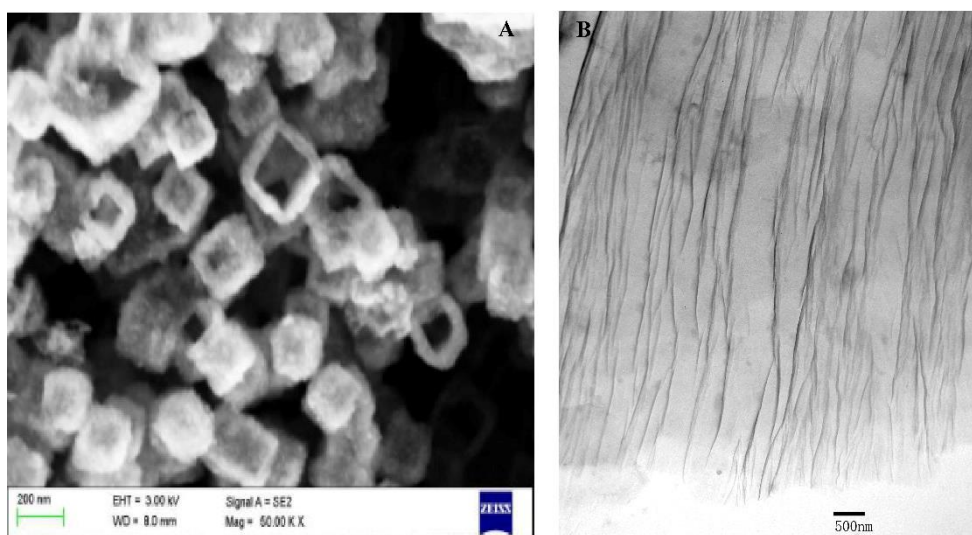


**Figure 1.** SEM image of CNCs and TEM image of rGO.

Fig. 1 A shows the morphology of carbon nanocages (CNCs) under scanning electron microscopy (SEM). The CNCs are a cubic cage structure with a diameter of 100-200 nm, and most of them are open structures. This structure significantly increases the specific surface area of CNCs. Fig. 1 B shows the transmission electron microscopy (TEM) diagram of rGO. In the figure, we can clearly see the reduced graphene oxide with a thin layer in the form of a folded structure, which can also increase the specific surface area of nanomaterials.

#### 3.2. Electrochemical characterization of CNCs/GCE

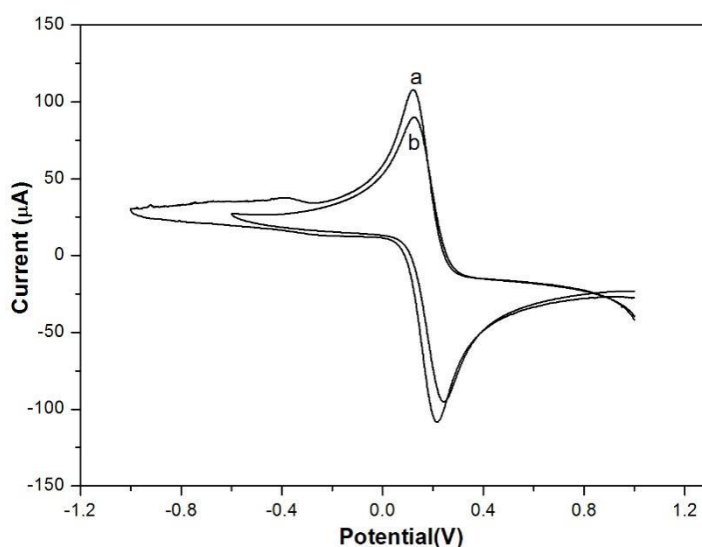


**Figure 2.** The cyclic voltammetric (CV) responses of the CNCs/GCE (a) and rGO/GCE (b) achieved in 50 mM potassium ferricyanide solution in 0.05 mol L<sup>-1</sup> PBS (pH 7.0). Scan rate, 50 mVs<sup>-1</sup>.

The modified electrode was characterized by cyclic voltammetry in 50 mM potassium ferricyanide solution at a scan rate of  $50 \text{ mV s}^{-1}$ . Fig. 2 shows that the CNCs/GCE has a better redox peak than the GCE in terms of peak current ( $I_p$ ) and peak separation ( $\Delta E_p$ ). The peak currents of CNCs/GCE are much larger than those of rGO/GC, which is mainly attributed to the electroactivity of the CNCs nanomaterials. The magnitudes of peak potential separation were 94 mV and 102 mV for CNCs/GCE and rGO/GCE, respectively. The former was much closer to the expected value (60 mV) for a reversible one-electron process, revealing the facilitated electrontransfer of  $[\text{Fe}(\text{CN})_6]^{4-}/[\text{Fe}(\text{CN})_6]^{3-}$  at the CNCs/GC electrode.

### 3.3. EIS characterization of CNCs/GCE

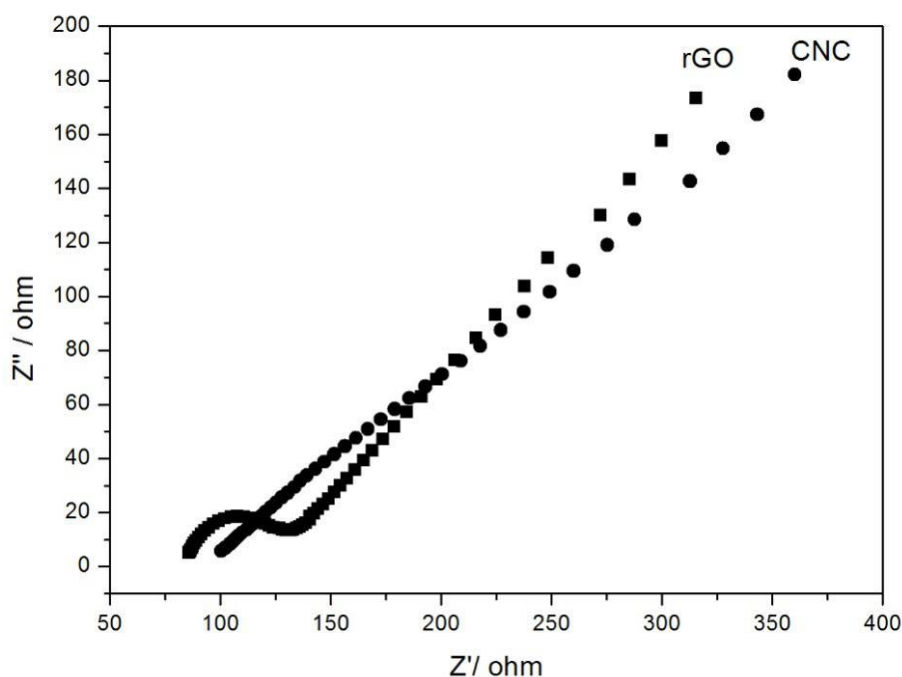


**Figure 3.** The EIS characterization of CNCs and rGO.

Electrochemical impedance spectroscopy (EIS) is an effective method to characterize the electrochemical process at the solution-electrode interface. The surface electron transfer resistance, which is equal to the diameter of the semicircle in the spectrum, can be used to describe the interface characteristics of the electrode. According to the calculation, the charge-transfer resistance ( $R_{ct}$ ) for rGO/GCE is  $86.85 \Omega$ , while that for CNCs/GCE is  $37.83 \Omega$ . This result is similar to that of mesoporous carbon nanomaterials in previous studies[13]. From these data, we can see that the resistance of carbon nanocages is lower and the charge transfer rate is faster, which better verifies the results in Fig. 2.

## 3.4 Kinetic characteristics of the CNCs/GC electrode

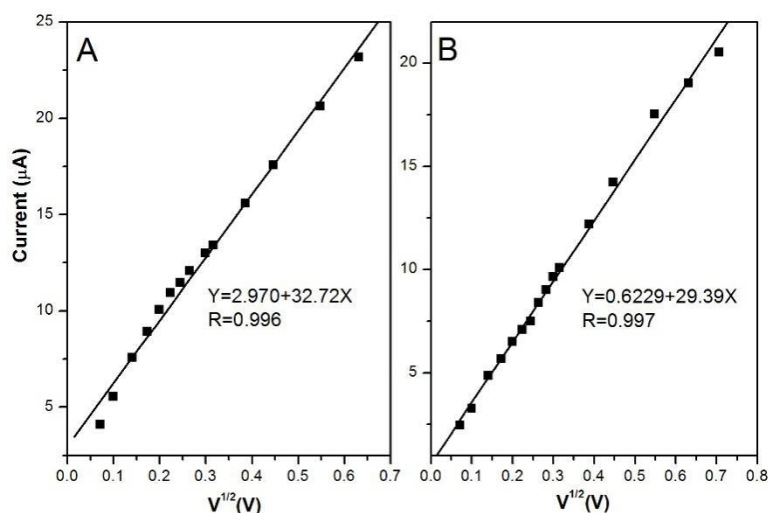


**Figure 4.** The peak current vs. the square root of the scan rate of 50 mM potassium ferricyanide detected at CNCs/GCE (a) and rGO/GCE (b) at different scan rates (10–400 mV)

To study the dynamic behavior of the two electrodes, the changes in the scan rate and peak current were measured. As shown in Fig. 4, the peak current will increase with increasing scan rate, and the peak current is proportional to the square root of the scan rate on both electrodes. The electrochemical area of the electrode can be calculated by the Randles–Sevcik formula,  $I_p = 2.69 \times 10^{-5} A D^{1/2} n^{3/2} V^{1/2} C$ , where  $D = 6.70 \times 10^{-6} \text{ cm}^2/\text{s}$  [14],  $n = 1$ , and  $C = 5 \text{ mM}$ . Given the slope of the straight line,  $A_{\text{CNCs}} = 0.0940 \text{ cm}^2$  and  $A_{\text{rGO}} = 0.0844 \text{ cm}^2$  can be calculated. This indicates that CNCs have a higher specific surface area and surface roughness than rGO. The electrochemical area of CNCs/GC is similar to that of mesoporous carbon nanomaterial-modified glass carbon electrodes, and both are larger than carbon nanotube-modified electrodes in previous studies [13].

## 3.4. Electrocatalytic oxidation of NADH

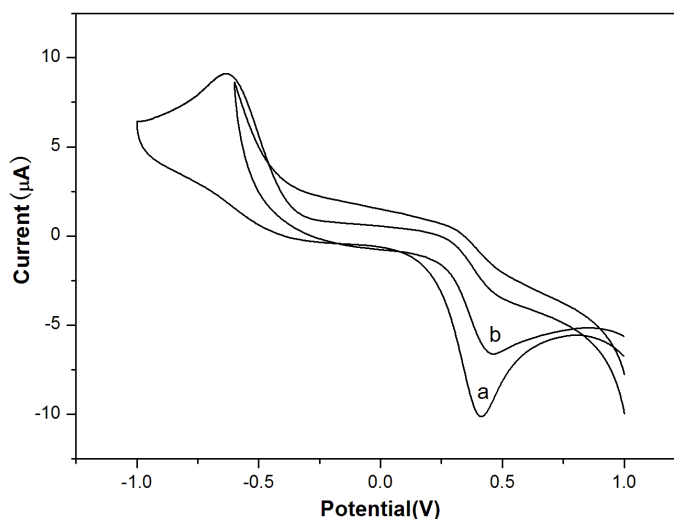


**Figure 5.** Cyclic voltammograms for the CNCs/GCE (a) and rGO/GCE (b) recorded in 1.0 mM NADH in phosphate buffer (pH 7.0,  $0.05 \text{ mol L}^{-1}$ ). Scan rate,  $50 \text{ mV s}^{-1}$ .

To compare the potential electrochemical properties of the two modified electrodes, the cyclic voltammetry of the two electrodes was compared in 1 mM NADH PBS buffer solution. Fig.5 shows that the peak current of the cathode decreases significantly at both electrodes, and the CNCs/GCE has a lower anodic peak current. The anodic peak potential at CNCs/GCE is 0.41 V while the peak potential at rGO/GCE is 0.47 V. Although CNCs and rGO both have electrocatalytic activities towards the oxidation of NADH, CNCs/GCE shows better electrocatalytic activity than rGO/GCE in terms of a higher peak current and more negative oxidation potential.

### 3.4. Amperometric NADH Biosensor

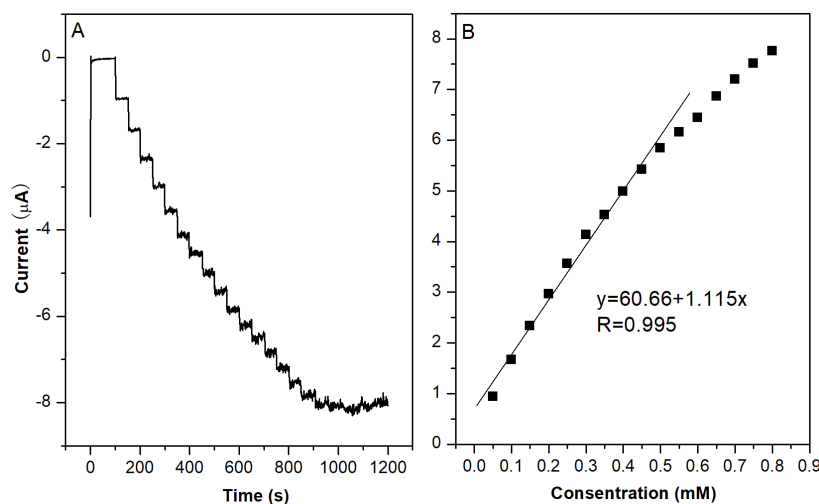


**Figure 6.** (A) Current-time responses for the rGO/GCE (a) and CNCs/GCE (b) with successive additions of 50 μM NADH. (B) Calibration curves for NADH at the rGO/GCE (a) and CNCs/GCE (b). Phosphate buffer solutions: pH 7.0, 0.05 M; Operation potential: 0.2 V.

Under the potential oxidation of NADH, the analytical performance of different electrodes for NADH was studied. Fig.6 shows the current-time response of CNCs/GCE and rGO/GCE at a working potential of 0.2 V. A concentration of 50 μM NADH was continuously added dropwise to a phosphate buffer solution (pH 7.0, 0.05 M) at intervals of 50 s. Each time the sample is added, the reaction at the CNCs/GC electrode reaches dynamic equilibrium within 4 seconds, while it takes 10 seconds at the rGO/GCE. The B diagram is a corresponding concentration-current standard curve. According to the standard curve, the electrode parameters of the corresponding electrode can be calculated. The detection limit, based on a signal-to-noise ratio of 3, is calculated as 0.34 μM, the linear range is up to 450 μM, and the sensitivity is 15.78 μA·μM<sup>-1</sup>·cm<sup>-2</sup>. The sensitivity and linear range results are better than those from our previous study[15]. Under the same experimental conditions, the linear relationship of NADH catalyzed by rGO/GCE is studied. At 0.2 V, the response current of rGO/GCE to NADH is very small, and the linear range is very narrow. The detection limit was calculated as 0.55 μM, the linear range was from 2.23 μM to 250 μM, and the sensitivity was 0.574 μA·μM<sup>-1</sup>·cm<sup>-2</sup>. After comparison, it is known that CNCs/GCE has a lower detection limit than rGO/GCE-catalyzed NADH, with a wider linear range and higher sensitivity.

### 3.5 Amperometric Ethanol Biosensor

As mentioned above, CNCs/GCE have good electrocatalytic performance for the oxidation of NADH, so CNCs/GCE can be used as a biological platform for the preparation of electrochemical biosensors based on dehydrogenase. Here, we chose alcohol dehydrogenase (ADH) as an example. ADH was immobilized on the surface of CNCs/GCE to prepare an ethanol biosensor (ADH/CNCs/GCE). The principle of the amperometric biosensor is as follows: ethanol is oxidized to acetaldehyde by nicotinamide adenine dinucleotide (oxidized state,  $NAD^+$ ). The coenzyme is necessary to receive ethanol electrons with the aid of ADH. At the same time,  $NAD^+$  is reduced to NADH, which can be regenerated and effectively recovered by releasing electrons and protons on the CNC/GCElectrode.



Therefore, the concentration of ethanol can be determined quantitatively by measuring the anodic current related to NADH oxidation on CNCs/GCE.

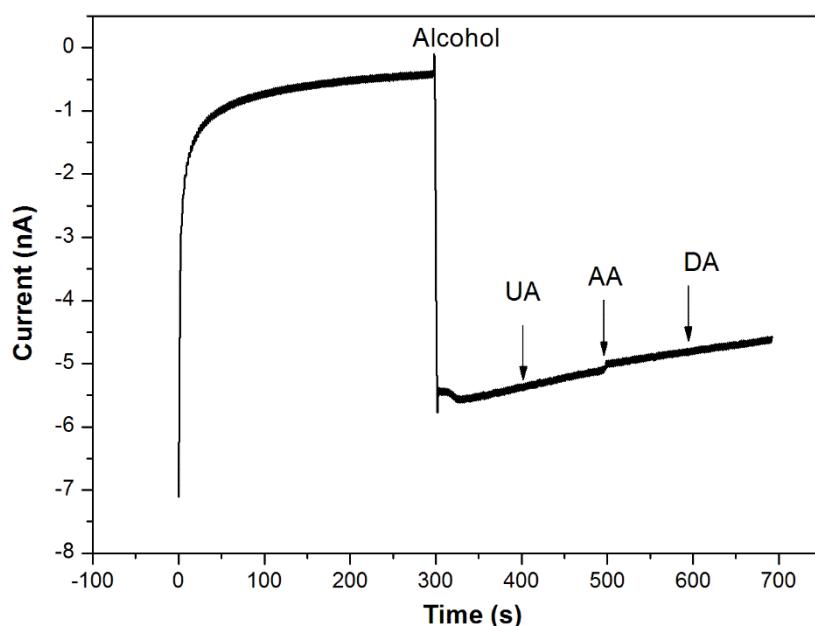


**Figure 7.** Amperometric response of the CNCs/GCE in phosphate buffer solutions (pH 7.0, 0.05 M) containing 1.0 mM ethanol spiked with DA (0.10 mM), UA (0.10 mM) and AA (0.10 mM)

The selection of the operation potential was carried out by the amperometric measurement of 1 mM ethanol spiked with 0.1 mM DA, 0.1 mM UA and 0.1 mM AA under an operational potential of 0.2V. After the response current was stabilized, 0.1 mM DA, 0.1 mM UA, and 0.1 mM AA were sequentially added. As shown in Fig.7, in all cases, UA, DA and AA showed no obvious interference with ethanol, and the response of ethanol still maintained a high sensitivity. Thus, the operation potential of 0.2 V was adopted for further studies.

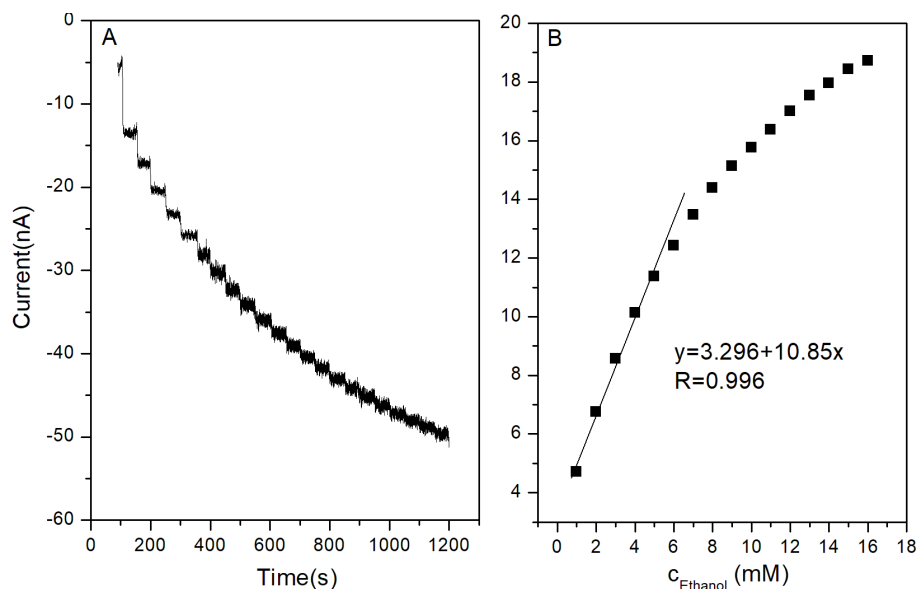


**Figure 8.** A Current – time responses for the CNCs/GCE with successive additions of 1 mM ethanol. B Calibration curves for ethanol at the ADH/CNCs/GCE. Phosphate buffer solution conditions: pH 7.0, 0.05 M, and 5 mM NAD<sup>+</sup>; Operation potential:0.2 V.

**Table 1.** Comparison between the proposed ADH/CNCs/GCE and other reported ethanol amperometric sensors from literature.

Electrode	Sensitivity	Linear range	Detection limit (μM)	Refs.
CPE NINWs	1372 μA /M	10 to 100 μM	0.31	[16]
Rosmarinic acid /ADH	1360 μA /M	23~ 1000 μM	23	[17]
ADH/MB/OMC/GCE	34.58 nA /mM	~6 mM	19.1	[18]
ADH/CNCs/GCE	10.85 nA /mM	~5 mM	300	This work

Fig.8 shows the amperometric response for successive additions of 1.0 mM ethanol to a stirred phosphate buffer (pH 7.0, 0.050 M) containing 5 mM NAD<sup>+</sup> at an operating potential of 0.2 V, and the corresponding calibration curve was recorded at ADH/CNCs/GCE. Each addition of ethanol causes the background current to rise rapidly and produce a steady-state response within 15 s. The sensitivity is 10.85 nA/mM. The linear response range of the biosensor is 5.0 mM, and the detection limit is 0.30 mM (S/N = 3).The detection data were not good except for the linear range compared with that of the similar amperometric sensors. The comparison data are listed in Table 1. According to the Lineweaver-Burk equation, the apparent Michaelis-Menten constant (kappM) of the ethanol biosensor is 2.41 mM. This value is similar to the previous report [17]. In addition, we measured the

reproducibility and repeatability of the ethanol biosensor. The relative standard deviation (RSD) was approximately 7.8% for the detection of a 1 mM ethanol solution with five bioelectrodes prepared by the same method and 5.8% for 10 measurements with a single bioelectrode.

**Table 2.** Determination of ethanol in serum samples with the ethanol

Sample No.	Blank serum (mM)	Added (mM)	Found (mM)	RSD (%)	Recovery (%)
1	0.00		0.00		
		1.00	0.92	4.81	91.90
2	0.00		0.00		
		1.00	0.93	4.54	92.80
3	0.00		0.00		
		1.00	0.92	5.32	92.30

The working stability and long-term stability (shelf life) of the ethanol biosensor were studied. ADH/CNCs/GCE was added to a 1 mM ethanol solution containing 5 mM  $\text{NAD}^+$  to study the operational stability of ADH/CNCs/GCE for 10 hours. The current response decreased by only approximately 12% in the first 2 hours and 23% in 10 hours, indicating that the electrode has good operational stability and can be used continuously for several hours.

The ethanol biosensor was applied to determine the concentration of ethanol in human serum samples to illustrate its practical application. Serum samples were provided by Jining Blood Center and diluted with phosphate buffer 10 times before determination. No ethanol was detected in these serum samples. Therefore, the standard addition method was used to verify the detection of ethanol in actual samples. Table 2 shows the recovery and RSD values for each of the three parallel assays. The results show that the recovery rate of this method is higher than 91%.

#### 4. CONCLUSIONS

Carbon nanocages were applied in electrochemical biosensors and displayed good electrocatalytic activities for NADH oxidation. An amperometric ethanol biosensor with relatively good sensitivity and selectivity was successfully prepared by combining alcohol dehydrogenase with a carbon nanocage. The ethanol biosensor was applied to the determination of ethanol concentration in human serum samples and showed high recovery.

## ACKNOWLEDGEMENTS

The authors are profoundly grateful for the financial support provided by Natural Science Foundation of Shandong province (No. ZR2019PB026, No. ZR2019PB019, No. ZR2018PB011, No. ZR2017BB015, No. ZR2015BL007), NSFC cultivation project of Jining Medical University(No. JYP20418KJ17, JYP2018KJ03 ) and College students innovations project of Shandong province (No.S201910443033).

## References

1. S. Qian, Z. Wei and Z. Wenliang , *Am. J. Physiol. Gastrointest. Liver. Physiol.*, 310 (2016) 205.
2. H. Derick, D. Maria and S. Heather, *J. Bio. Chem.*, 287 (2012) 42165.
3. A. Ahmed, *Biomark. Med*, 4 (2010) 241.
4. W. Shaogui, P. Pal and C. Robert, *Alcohol. Clin. Exp. Res.*, 40 (2016) 1215.
5. O. V. Pupysheva, A. A. Farajian and B. I. Yakobson, *Nano letters*, 8 (2007) 767.
6. A. Vinu, M. Miyahara and V. Sivamurugan, *J. Mater. Chem.*, 15 (2005) 5122.
7. I. Gill, A. Ballesteros, *J. Am. Chem. Soc.*, 120 (1998) 8587.
8. M. Tadokoro, S. Tsumeda and N. Tshara, *J. Nanosci. Nanotechno.*, 9 (2009) 391.
9. Y. Tan, C. Xu and G. Chen , *ACS Appl. Mater. Inter.*, 5 (2013) 2241.
10. K. Xie, X. Qin and X. Wang, Wang Y, *Adv. Mater.*, 24 (2012) 347.
11. Z. M. Sheng, C. X. Guo and C. M. Li, *Electrochem. Commun.*, 19 (2012) 77.
12. L. Jiang , J. Wang , X. Mao, *Carbon*, 111 (2017) 207.
13. M Zhou, J Guo, L.P Guo and J Bai, *Anal. Chem.*, 80 (2008) 4642.
14. X. Gao, W. Wei, L. Yang, *Electroanalysis*, 18 (2006) 485.
15. X Mao, X Wang, X Xu and L Jiang. *Int. J. Electrochem. Sci.*, 15 (2020) 6425.
16. C.S. Tettamanti, M.L. Ramírez and F.A. Gutierrez, *Microchem. J.*, 142 (2018) 159.
17. M. Bilgi, E.M. Sahin and E. Ayrançi, *J. Electroanal. Chem.*, 813 (2018) 67.
18. X. Jiang , L. Zhu and D. Yang, *Electroanalysis*, 21 (2009) 1617.

© 2021 The Authors. Published by ESG ([www.electrochemsci.org](http://www.electrochemsci.org)). This article is an open access article distributed under the terms and conditions of the Creative Commons Attribution license (<http://creativecommons.org/licenses/by/4.0/>).